Rev. Adv. Mater. Sci. 28 (2011) 141-144

CHEMICAL VAPOR TRANSPORT PROCESS IN HYDROGEN REDUCTION OF BALL-MILLED MOLYBDENUM AND TUNGSTEN OXIDE POWDERS

Se Hoon Kim, Dae-Gun Kim, Young Ik Seo and Young Do Kim

Department of Materials Science and Engineering, Hanyang University, Seoul 133-791, Korea

Received: February 17, 2011

Abstract. Chemical vapor transport of ball-milled MoO_3 and WO_3 powders in a non-isothermal hydrogen reduction process was discussed in terms of the sizes and specific surface area of oxide particles. Although all reduction processes were completed at nearly the same temperature, they became stepwise with lower starting temperatures and peak points of each sequence due to the refinement of the oxide particles. In particular, the chemical vapor transport process in the reduction of MoO_3 ($MoO_3 \rightarrow MoO_2$) was strongly affected by the initial states of the oxide powders.

1. INTRODUCTION

The hydrogen reduction processes of molybdenum (Mo) and tungsten (W) oxides include chemical vapor transport (CVT), which consists of a three-stage reaction: formation of the volatile Mo or W hydrates through a surface reaction with water vapor, transport of the hydrates, and reduction of the volatile hydrates to elemental materials at the surface of the growing oxide [1-7]. It is interesting to note that the CVT process of each oxide takes place in different reaction steps. In the case of Mo oxide, it takes place in the first step of the reaction $MoO_3 \rightarrow MoO_2$, while for W oxide it takes place in the second stage of $WO_2 \rightarrow W$ [3,4,6-8]. This CVT process is strongly dominated by the change in localized humidity, which is closely related to the condition of the oxide powder bed [2,5,7]. For both oxides, the CVT process in hydrogen reduction has been discussed in relation to a mechanochemical process to fabricate nanostructured metal and nanocomposite powders [4,6,8,9]. However, more detailed studies of the individual system are required to control the final metal products from the elemental oxide powders. In this study, the CVT process of ball-milled MoO_3 and WO_3 powders in a non-isothermal hydrogen reduction process was discussed in terms of the sizes and specific surface areas of the oxide particles.

2. EXPERIMENTAL PROCEDURE

MoO_3 (Kojundo Chemical Lab. Co., 4.69 μm, 99.9%, JAPAN) and WO_3 (TaeguTec Co., 20 μm, 99.95%, KOREA) powders were used as raw materials. Each prepared oxide powder was ball-milled at 400 rpm for up to 50 h using an attritor. The jar (2 l) and the ball (5 mm) for ball-milling were made of stainless steel, and the ball-to-powder ratio was 16:1. Ball-milled MoO_3 and WO_3 powders were reduced under non-isothermal conditions at up to 800 and 1000 °C, respectively, at a heating rate of 10°C/min in a hydrogen atmosphere with a –76 °C dew point. The water vapor content in the outlet gas resulting from the hydrogen reduction of the oxides was measured with an *in situ* humidity measuring system. The Brunauer-Emmett-Teller (BET) method and scanning electron microscopy (SEM) were employed to ana-

Corresponding author: Y.D. Kim, e-mail: ydkim1@hanyang.ac.kr

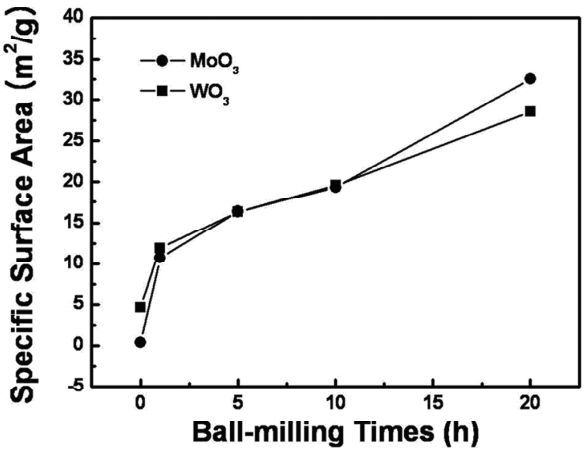

Fig. 1. Specific surface area changes in MoO_3 and WO_3 powder with various ball-milling times.

lyze the microstructural characteristics of the powders.

3. RESULTS AND DISCUSSION

Ball-milling refines the oxide powders, so that the specific surface area increases with ball-milling time. Further, the pore structure of the powder bed on the micrometer scale becomes complicated with micro-, submicro-, and nano-sized pore networks. As we previously reported [3,4], the crystalline sizes of MoO_3 and WO_3 ball-milled for 20 h reached 10-20 nm. Fig. 1 depicts the changes in specific surface area of MoO_3 and WO_3 powders as a result of the ball-milling process. At the initial stage of ball-milling, the reduction in the specific surface area was very large, and it increased nearly linearly with increased ball-milling time.

The increased surface areas of the oxide powders were expected to strongly influence their hydrogen-reduction behaviors. Fig. 2a shows the non-isothermal humidity curves for the heating of (powder ball-milled) MoO_3 for various times at a 10 °C/min heating rate under a hydrogen atmosphere and the corresponding humidity peak temperatures. The change in humidity in the outlet gas was assumed to be a result of the hydrogen reduction process according to the overall reaction. As shown in Fig. 2a, there are two reactions for the hydrogen reduction of MoO_3, as illustrated by the two humidity peaks. The two reactions take place in two distinct stages, viz.: $MoO_3 + H_2 \rightarrow MoO_2 + H_2O$ (1) and $MoO_2 + 2H_2 \rightarrow Mo + 2H_2O$ (2) [1,2,10]. The first reaction is assigned to the reduction process of $MoO_3 \rightarrow MoO_2$, occurring over a temperature range of 450-650 °C. Below 450 °C, the reduction process proceeds very slowly, yielding intermediate oxides of Mo_4O_{11} between MoO_3 and MoO_2. The second reaction, which occurs in the temperature range of 650-800 °C, is assigned to the reduction process of $MoO_2 \rightarrow Mo$. These reactions took place as the temperature decreased with increased ball-milling, although the final reduction process was complete

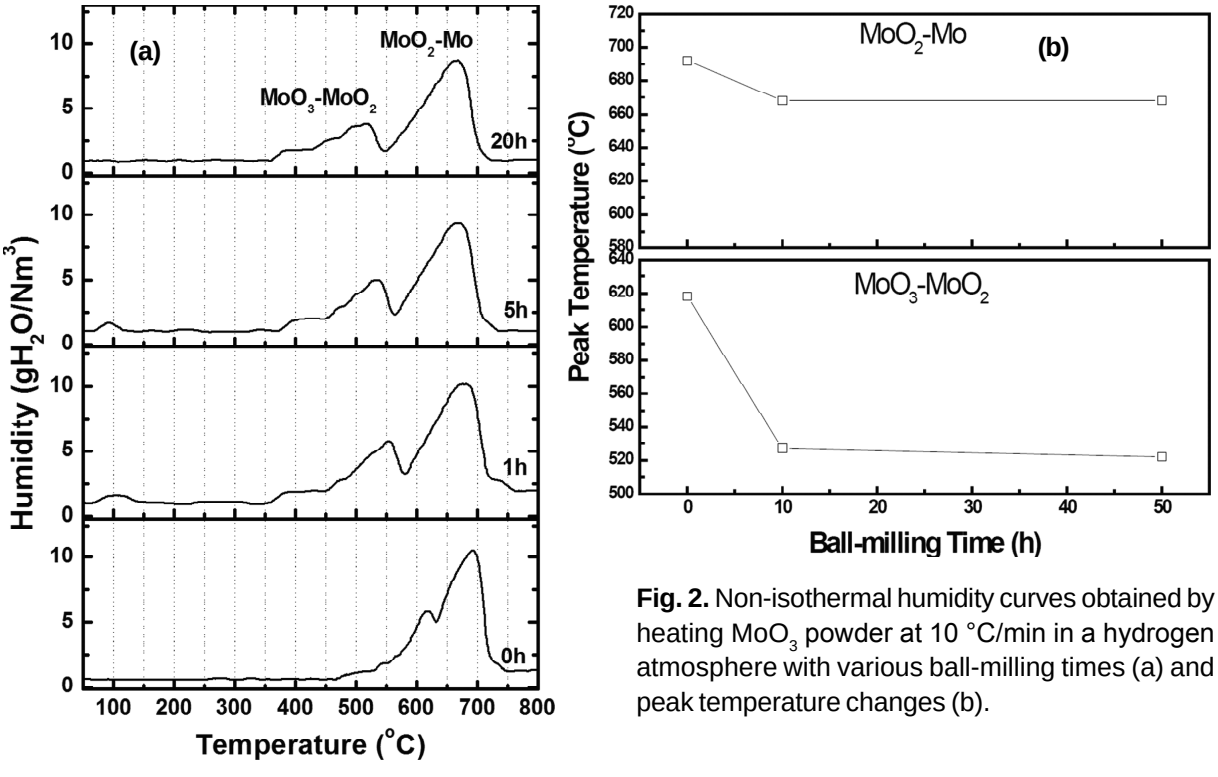

Fig. 2. Non-isothermal humidity curves obtained by heating MoO_3 powder at 10 °C/min in a hydrogen atmosphere with various ball-milling times (a) and peak temperature changes (b).

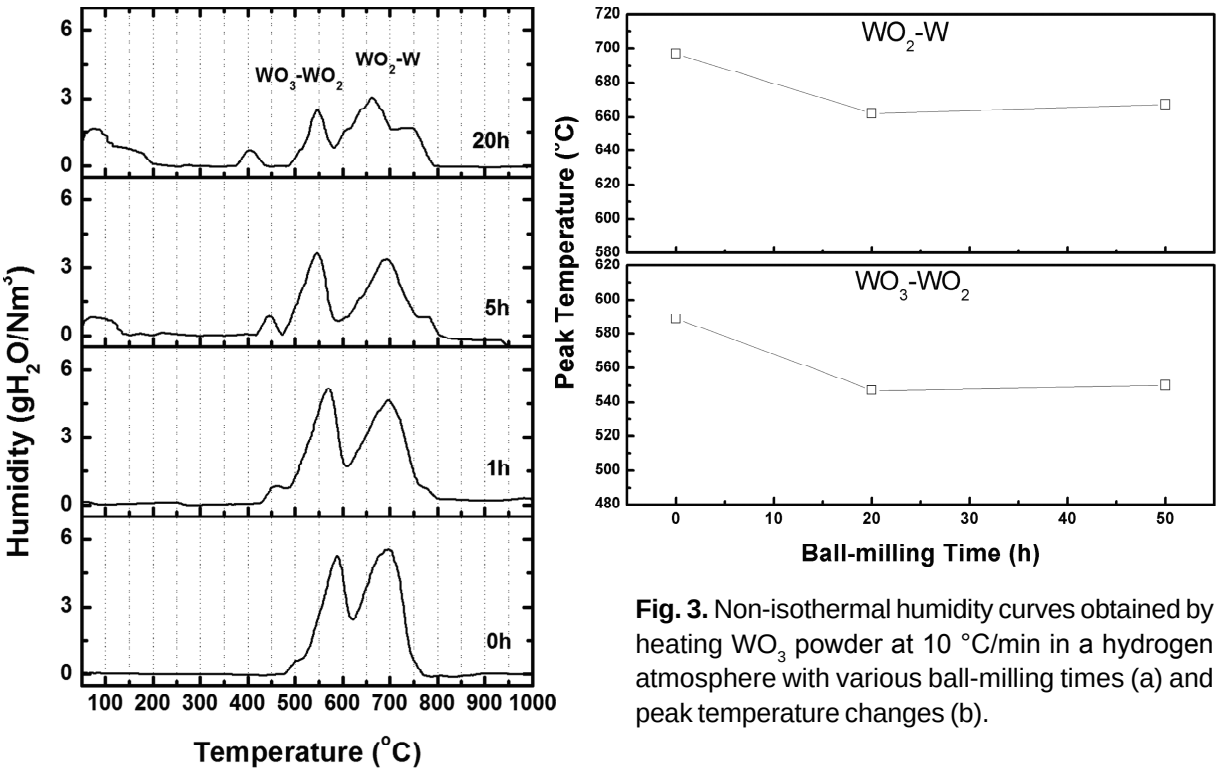

Fig. 3. Non-isothermal humidity curves obtained by heating WO_3 powder at 10 °C/min in a hydrogen atmosphere with various ball-milling times (a) and peak temperature changes (b).

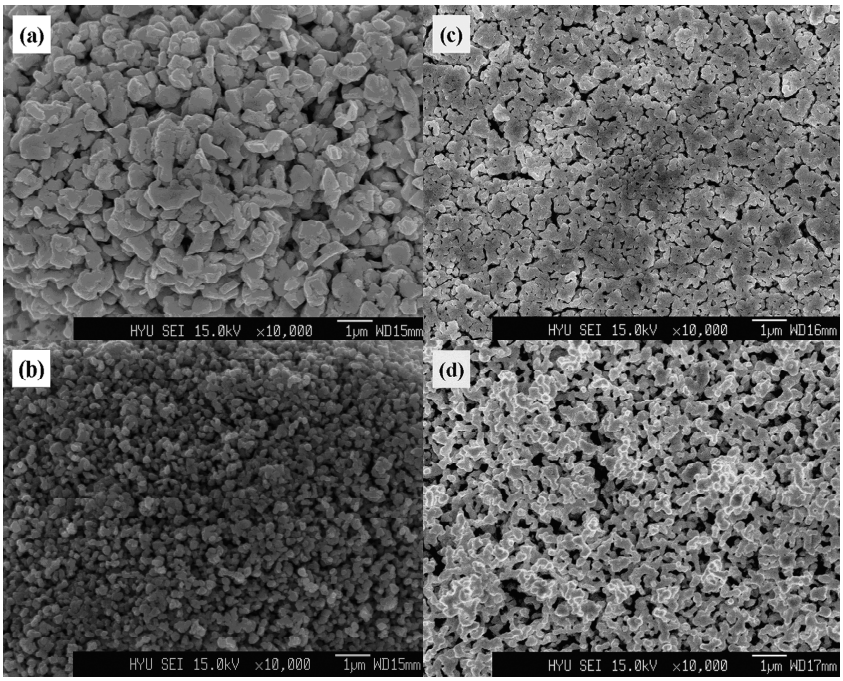

Fig. 4. Micrographs of hydrogen-reduced Mo (a, b) and W (c, d) powder ball-milled for 0 h (a, c), 20 h (b), and 10 h (d).

at the nearly same temperature, around 750 °C. In the first reaction of $MoO_3 \rightarrow MoO_2$, which was dominated by CVT [2,3], the starting temperature, the peak, and the finishing temperatures were decreased stepwise over a range of 200 °C from 350 °C to 550 °C due to ball-milling. The second reaction, $MoO_2 \rightarrow Mo$, governed by oxygen transport occurred at a considerably lower temperature, covering a wide temperature range after ball-milling. The change in the peak temperature by ball-milling was small compared with that of the first reaction. Such changes in peak temperature are presented in Fig. 2b. The extended surface areas of the ball-milled oxide powders induced a decrease in the starting temperature by enhancing oxygen transport at the initial stage of CVT. In the case of ball-milled oxide, the

supply of H_2 and the removal of H_2O resulting from the reduction were transported easily through the pore network formed by ball-milling. Consequently, the hydrogen reduction of the ball-milled MoO_3 powder by CVT in the first step could be slow and stepwise compared with that of the micro-sized elemental oxide powder. Also, the reduction by CVT could be more sensitive to particle size and pore structure than reduction by oxygen transport through the solid phase, because of the diffusion of the gas phase during the CVT process (Fig. 2b).

Fig. 3a indicates the non-isothermal humidity curves for the hydrogen reduction of WO_3 powders according to the overall reaction with two reduction stages. Both reactions take place in two distinct stages, viz.: $WO_3 + H_2 \rightarrow WO_2 + H_2O$ (1) and $WO_2 + 2H_2 \rightarrow W + 2H_2O$ (2) [4,5,7,11]. As mentioned above, the CVT process dominates the $WO_2 \rightarrow W$ stage, in contrast with the hydrogen reduction of the Mo oxide. The reduction step $WO_3 \rightarrow WO_2$, which was dominated by oxygen transport, also became noticeably slower and stepwise in the reaction $MoO_3 \rightarrow MoO_2$ by CVT; moreover, the peak temperature shifted to a lower temperature because of the surface extension by ball-milling. The shift in peak temperatures for the CVT process of W oxide, however, was not as insignificant as that of Mo oxide, as shown in Fig. 3b. This was because the CVT process dominates the $WO_2 \rightarrow W$ step at a high temperature. Because the hydrogen reduction of the $WO_3 \rightarrow WO_2$ stage accompanied grain growth, the effect of ball-milling on particle size refinement may have been somewhat reduced prior to the CVT process.

After the hydrogen reduction process, a relatively coarse Mo powder could be obtained from micro-sized MoO_3 elemental powder without ball-milling. Fig. 4 presents the morphologies of reduced powder. The raw MoO_3 powder was loosened, and its initial shape was changed as depicted in Figs. 4a and 4b. In the case of raw WO_3 powder without ball-milling, the powder morphology of elemental WO_3 was maintained after the reduction process; the powder consisted of small W metal grains within a large particle as presented in Figs. 4c and 4d. This difference depended upon whether the CVT process occurred at the initial stage of reduction. Moreover, the particle size of the reduced metal phase was strongly affected by the ball-milling process in the case of Mo because of the lower temperatures of the CVT process.

4. CONCLUSIONS

The starting temperatures of hydrogen reduction were increased by the ball-milling process in both oxides because of refinements in particle size and increases in specific surface area. Also, the CVT became stepwise with ball-milling. The CVT of each oxide occurs at a different reaction step, i.e., the first step ($MoO_3 \rightarrow MoO_2$) of hydrogen reduction for the Mo oxide and the second step ($WO_2 \rightarrow W$) for the W oxide. In particular, the peak temperature for the $MoO_3 \rightarrow MoO_2$ reaction was remarkably decreased compared to that of the W oxide because the effect of particle size refinement would be stronger at the lower temperatures of the CVT for the Mo oxide than at the higher temperatures for the W oxide.

ACKNOWLEDGMENT

This work supported by a research fund of the Ministry of Education, Science and Technology (MEST), Korea (2009-0075831).

REFERENCES

[1] M.J. Kennedy and S.C. Bevan // *J. Less-Common Met.* **36** (1974) 23.
[2] V.S. Werner and M.O. Hugo // *Int. J. Refract. Met. Hard Mater.* **20** (2002) 261.
[3] G.S. Kim, Y.J. Lee, D.G. Kim and Y.D. Kim // *J. Alloys Compd.* **454** (2007) 327.
[4] D.G. Kim, K.H. Min, S.Y. Chang, S.T. Oh, C.H. Lee and Y.D. Kim // *Mater. Sci. Eng. A* **399** (2005) 326.
[5] E. Lassner and W.D. Schubert, *Tungsten* (Kluwer Academic/Plenum Press, New York, 1999).
[6] G.S. Kim, Y.J. Lee, D.G. Kim, S.T. Oh, D.S. Kim and Y.D. Kim // *J. Alloys Compd.* **419** (2006) 262.
[7] W.D. Schubert // *J. Refract. Met. Hard Mater.* **4** (1990) 178.
[8] T.H. Kim, J.H. Yu, and J.S. Lee // *Nanostruct. Mater.* **9** (1997) 213.
[9] D.G. Kim, S.T. Oh, H.T. Joen, C.H. Lee and Y.D. Kim // *J. Alloys Compd.* **354** (2003) 239.
[10] E.R. Braithwaite and J. Haber, *Molybdenum-An Outline of its Chemistry and Uses* (Elsevier, New York, 1994).
[11] M. Hashempour, H. Razavizadeh, H.R. Rezaie and M.T. Salehi // *Mater. Charact.* **60** (2009) 1232.